Title	Orbital ordering and two ferromagnetic phases in low-doped La 1-xSr xMnO 3
Author(s)	Shen, SQ; Gu, RY; Wang, QH; Wang, ZD; Xie, XC
Citation	Physical Review B - Condensed Matter And Materials Physics, 2000, v. 62 n. 9, p. 5829-5833
Issued Date	2000
URL	http://hdl.handle.net/10722/43298
Rights	Physical Review B (Condensed Matter and Materials Physics). Copyright © American Physical Society.

Orbital ordering and two ferromagnetic phases in low-doped $La_{1-x}Sr_xMnO_3$

Shun-Qing Shen,[1,2] R. Y. Gu,[1] Qiang-Hua Wang,[3] Z. D. Wang,[1] and X. C. Xie[4]
[1]*Department of Physics, The University of Hong Kong, Pokfulam, Hong Kong, China*
[2]*Institute of Physics, Chinese Academy of Sciences, P.O. Box 603, Beijing 100080, China*
[3]*Department of Physics and National Laboratory of Solid State Microstructures, Nanjing University, Nanjing 210093, China*
[4]*Department of Physics, Okalahoma State University, Stillwater, Oklahoma 74078*
(Received 13 January 2000; revised manuscript received 1 June 2000)

We present a theory for the transition between two ferromagnetic phases observed experimentally in lightly doped $La_{1-x}Sr_xMnO_3$. Starting from an electronic model, the instabilities to various types of orbital orderings are studied within the random-phase approximation. In most cases, the instabilities occur in the region of strong correlations. A phase diagram is calculated in the case of strong correlation by means of the projected perturbation technique and the Schwinger boson technique. A phase transition between two types of orbital ordering occurs at a low doping, which may be closely relevant to recent experimental observations.

I. INTRODUCTION

Doped manganites have attracted much current research interest due to various types of charge, orbital and magnetic orderings, as well as the colossal magnetoresistance effect. It was observed experimentally that a phase transition occurs at $T=150$ K in slightly doped manganite $La_{1-x}Sr_xMnO_3$ ($x=\frac{1}{8}$) from a ferromagnetic metallic phase to a ferromagnetic insulating phase.[1–3] The low-temperature insulating phase is found to be stabilized by an external magnetic field. Alternatively, a ferromagnetic metallic state can evolve into a ferromagnetic insulating state by increasing an external magnetic field,[2] which is completely opposite to the field-induced melting of the charge-ordering phase near $x=\frac{1}{2}$.[4] On the other hand, at low temperatures, a metallic phase crosses over to an insulating phase near $x=0.175$.[5,6] Since the spin degrees of freedom have been frozen, the transition should be attributed to the orbital orderings of active e_g electrons in Mn ions. Theoretically, the phase diagrams of doped manganites have been investigated extensively.[7–15] The importance of the orbital ordering was realized to explain the layered-type antiferromagnetism for the undoped case and various types of magnetic orderings in the highly doped regime. Experimental evidence shows that the orbital ordering indeed exists in $LaMnO_3$ and $La_{0.5}Sr_{1.5}MnO_4$.[16] In this paper, we propose an electronic origin of the ferromagnetic phase transition, and emphasize the roles of orbital ordering and strong electron correlations. A Hubbard-type electronic model is presented to describe the orbital motions of active electrons in Mn ions, and the random-phase approximation (RPA) is applied to investigate the instability of various types of orbital structures. It is found that the para-orbital phase is unstable when the on-site Coulomb interaction is strong. In this case, we derive an effective Hamiltonian in the representation of the Schwinger boson for orbital and spinless fermions for charge. A phase transition between two types of orbital ordering phases is observed. Its relevance to the experimental observation is also discussed.

II. MODEL

Doped manganites are very complicated and contain a number of physical degrees of freedom. To simplify our problem, we only concentrate on the fully polarized ferromagnetic phase such that all spin degrees of freedom are frozen completely. Other interactions, such as the cooperative Jahn-Teller effect, are neglected in a fully saturated phase. Under these circumstances, the electronic Hamiltonian for the doped manganite might be written as[10]

$$H=-t\sum_{ij} c^{\dagger}_{i,\alpha}c_{j,\alpha}+\sum_i Un_{i,z}n_{i,\bar{z}},$$

where $c^{\dagger}_{i,\alpha}$ and $c_{i,\alpha}$ are the creation and annihilation operators for electrons in the α $(=x,y,z)$ orbital at site i. α is determined by the orientation of the difference **i-j**. The operators are not independent: $c_{i,x}=\frac{1}{2}c_{i,z}-(\sqrt{3}/2)c_{i,\bar{z}}$ and $c_{i,y}=\frac{1}{2}c_{i,z}+(\sqrt{3}/2)c_{i,\bar{z}}$. $c^{\dagger}_z|0\rangle=|z\rangle\propto(3z^2-r^2)/\sqrt{3}$ and $c^{\dagger}_{\bar{z}}|0\rangle=|\bar{z}\rangle\propto x^2-y^2$, respectively. Here the transfer matrices are assumed to take a Slater-Koster form given by the hybridization between the e_g orbital and the nearest oxygen p orbital.[17,18] U is the on-site Coulomb interaction for electrons at different orbitals with the same spin. Along any axis, the free electrons have two bands: one is $\omega(k)=-2t\cos k_a$, and the other is a flatband with $\omega(k)=0$. Since

$$n_{i,x}n_{i,\bar{x}}=n_{i,y}n_{i,\bar{y}}=n_{i,z}n_{i,\bar{z}},$$

which are the projection operators for double occupancy, the model can be regarded as a combination of three one-dimensional Falikov-Kimball models. When $U=0$, the spectra of free electrons are

$$\omega_{\pm}(k)=-t(e_x+e_y+e_z)\pm t\sqrt{e_x^2+e_y^2+e_z^2-e_xe_y-e_ye_z-e_ze_x},$$

where $e_\alpha=\cos k_\alpha$. The ground state is a para-orbital state for any doping. As the three $c_{i,\alpha}$ are not independent, one of the main features in the density of state in the Falicov-Kimball model, the peak for the localized electron, disappears.

III. THE RANDOM-PHASE APPROXIMATION

To further understand the physics of the model at low temperatures, we study the instability of the para-orbital

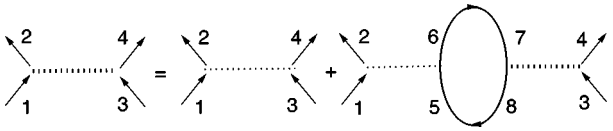

FIG. 1. Feynman diagram of the Dyson equations for the dressed interaction tensor. The numbers represent the orbital indices.

phase to various types of orbitally ordered phases in the random-phase approximation (RPA). As the Hamiltonian possesses the cubic symmetry, but lacks the SU(2) symmetry, the symmetry breaking is to choose a certain direction. We perform a unitary transformation

$$\begin{pmatrix} c_{i,z} \\ c_{i,z}^{-} \end{pmatrix} \Rightarrow R(\theta) \begin{pmatrix} c_{i,z} \\ c_{i,z}^{-} \end{pmatrix},$$

where

$$\mathbf{R}(\theta) = \begin{pmatrix} \cos\frac{\theta}{2} & \sin\frac{\theta}{2} \\ -\sin\frac{\theta}{2} & \cos\frac{\theta}{2} \end{pmatrix}$$

such that the hopping matrix depends on the angle θ while the on-site term remains unchanged in the new basis. However, such a unitary transformation does not change any physics of a system with SU(2) symmetry. In the new basis set, the various instabilities against the para-orbital state can be probed by the dressed 4×4 interaction tensor,

$$\mathbf{V}(q,\theta) = [1 - \mathbf{V}_0 \mathbf{\Pi}_0(q,\theta)]^{-1} \mathbf{V}_0,$$

as shown in Fig. 1. Here $\mathbf{V}_0$ is the bare interaction tensor that depends on the four orbital states, with two (leading to four combinations) at each end of the interaction line,

$$\mathbf{V}_0(\sigma_1\sigma_2;\sigma_3\sigma_4) = \frac{U}{2}\sigma_1\sigma_3(\delta_{\sigma_1\sigma_2}\delta_{\sigma_3\sigma_4} + \delta_{\sigma_1\sigma_4}\delta_{\sigma_2\sigma_3}),$$

where $\sigma_i = z(+1), \bar{z}(-1)$ denote the orbital states. $\Pi_0(q,\theta)$ is the polarization tensor, $q \equiv (\mathbf{q}, i\nu_n)$ with $\mathbf{q}$ the momentum transfer by the interaction, and ν_n is the bosonic Matsubara frequency. The 2×2 inverse of the free propagator matrix in our case is

$$\mathbf{G}^{-1}(k,\theta) = (i\omega_n + \mu)\mathbf{I} - \mathbf{R}^{-1}(\theta)\mathbf{E}(\mathbf{k})\mathbf{R}(\theta),$$

where $k \equiv (\mathbf{k}, i\omega_n)$ with ω_n being the fermionic Matsubara frequency and

$$\mathbf{E}(\mathbf{k}) = -t \begin{pmatrix} e_z + \frac{1}{4}(e_x + e_y) & -\frac{\sqrt{3}}{4}(e_x - e_y) \\ -\frac{\sqrt{3}}{4}(e_x - e_y) & \frac{3}{4}(e_x + e_y) \end{pmatrix}.$$

The polarization tensor is given by

$$\Pi_0(q,\theta)_{\sigma_1\sigma_2;\sigma_3\sigma_4} = -T\sum_{\omega_n} \int \frac{d^3\mathbf{k}}{(2\pi)^3} \times \mathbf{G}_{\sigma_2,\sigma_3}(k+q,\theta)\mathbf{G}_{\sigma_4,\sigma_1}(k,\theta),$$

where T is the temperature. The summation over fermion Matsubara frequencies can be easily performed, but the remaining integration over momenta has to be carried out numerically. By analytical continuation, we calculate the real-time zero-frequency limit of the dielectric tensor,

$$\varepsilon(\mathbf{q},0,\theta) = 1 - \lim_{w\to0} \mathbf{V}_0 \Pi_0(\mathbf{q}, i\nu_n \to \omega + i0^+, \theta).$$

At a specific wave number $\mathbf{q}$, the peak in the inverse of the determinant of the dielectric tensor, $1/\det[\varepsilon(\mathbf{q},0,\theta)]$, as a function of the on-site interaction U or temperature T, indicates the instability from the para-orbital ordering to some ordered phase at this wave number. For example, at $\mathbf{q} = (0,0,0)$, the peak indicates the instability to the polarized orbital (F) phase, $\mathbf{q} = (\pi,\pi,\pi)$ to the rock-salt (G) -type orbital ordering phase, $\mathbf{q} = (\pi,\pi,0)$ to the rod (C) -type orbital ordering, and $\mathbf{q} = (0,0,\pi)$ to the layered (A) -type orbital ordering. Numerical results of the zero-temperature critical on-site interaction U_c for the various orderings as a function

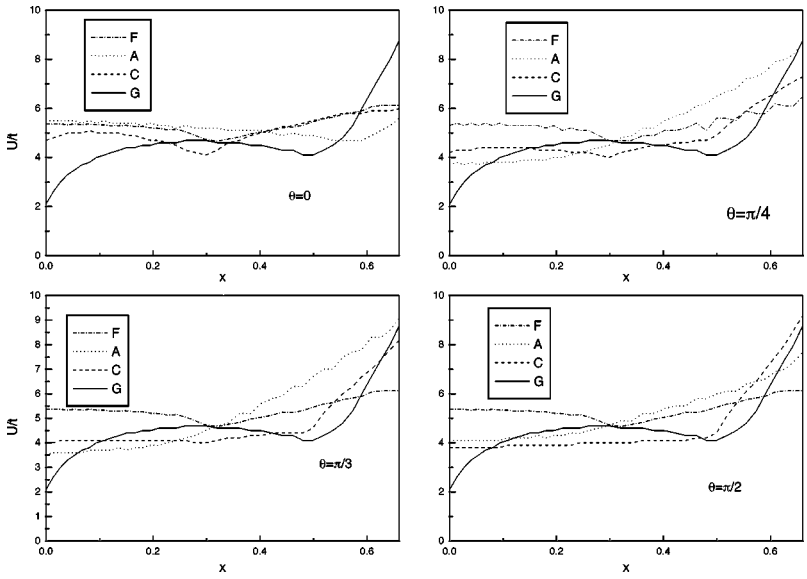

FIG. 2. Instablility of para-orbital phase to various ordering phases in the random-phase approximation.

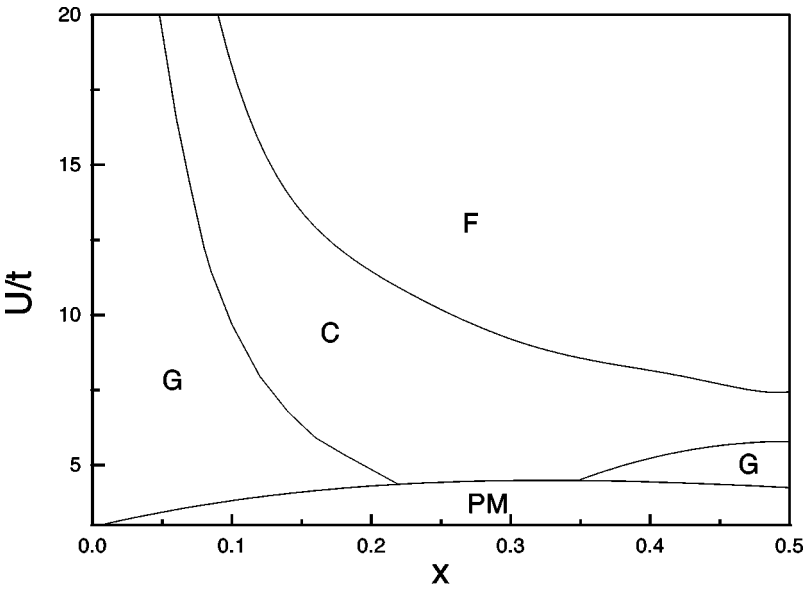

FIG. 3. The phase diagram for orbital ordering in low doped mangnites: the weak-correlation approach.

of the doping level for θ $(=0;\pi/4;\pi/3;\pi/2)$ are plotted in Fig. 2. It should be pointed out that for the G-type ordering, there is a logarithmic divergence in the polarization tensor, so that U_c approaches zero as $x\rightarrow 0$. However, it is difficult to capture this behavior by numerical calculations. Indeed, on a $100\times 100\times 100$ cubic lattice, we still get a finite U_c for the G-type ordering. Remarkably, $U_c(x)$ as a function of the hole concentration for the G-type is *not* a monotonic function of x, in contrast to that in the one-band Hubbard model. This difference arises solely from the existence of an orbital-flipping propagator in our system. The G-type ordering is not the unique stable phase when the doping or U increases. Other types of ordering also arise in some regimes. We find that the critical values U_c for G-type and F-type orderings are not sensitive to the change of angle θ while U_c for A-type and C-type are. The C-type ordering arises near $x=0.3$ for a moderate value of U, while an F-type ordering appears for high dopings. Figure 2 also shows that θ depends on the density of doping, especially for the A- and C-type orderings. As the instability in Fig. 2 can arise from the para-orbital phase against any ordered phases, the figure does not give us any information on which one is more stable in the large U limit. To obtain a phase diagram, a mean-field theory is introduced by decoupling

$$n_{i,z}n_{i,\bar{z}}\simeq\langle n_{i,z}\rangle n_{i,\bar{z}}+n_{i,z}\langle n_{i,\bar{z}}\rangle-\langle n_{i,z}\rangle\langle n_{i,\bar{z}}\rangle$$

and by setting

$$\frac{1}{2}\langle n_{i,z}-n_{i,\bar{z}}\rangle=e^{i\mathbf{q}\cdot\mathbf{r}_i}\Delta m_{\mathbf{q}},$$

where $\Delta m_{\mathbf{q}}$ is the order parameter for the ordered phase characterized by the momentum $\mathbf{q}$. Apart from $\Delta m_{\mathbf{q}}$, we also take θ as an additional variable. Again, we consider four types of orbital orderings: F, A, C, and G. The phase diagram in Fig. 3 is established by comparing the ground-state energies for different orderings, which is minimized in terms of $\Delta m_{\mathbf{q}}$ and θ.

IV. STRONG CORRELATION: SCHWINGER BOSON THEORY

From Fig. 2, the instabilities of several types of orbital ordering occur above $U\approx 5$ ($t=1$ is the energy unit), which can be regarded in a region of strong correlation since the on-site U is much larger than the bandwidth. On the other hand, from the estimation of excitation energies of Mn ions and the density-functional theory,[19,20] the ratio of t/U is estimated to be 0.1–0.05 . In this case, the double occupancy of electrons on the same site should be very sparse, and the projection perturbation technique is an efficient tool to investigate the low-energy physics in the model. Up to the second-order perturbation, we obtain an effective Hamiltonian:[15,21]

$$H=-\sum_{ij}\ t\tilde{c}^{\dagger}_{i,\alpha}\tilde{c}_{j,\alpha}-\sum_{ij}\ \frac{t^2}{U}n_{i,\alpha}n_{j,\bar{\alpha}}, \tag{1}$$

where $\tilde{c}^{\dagger}_{i,\alpha}$ and $\tilde{c}_{i,\alpha}$ indicates the exclusion of double occupancy on the same site. The physical meanings of the two terms in the effective Hamiltonian are very clear. Along any specific axis, the superexchange term is Ising-like, instead of the Heisenberg one that appeared in the usual t-J model. The total superexchange terms are a combination of three Ising models. Due to the fact that the orbital operators depend on the orientations of the bond, the physical properties are quite different from those of the usual Ising model as will be shown below. The C- and/or G-type orderings originate from the superexchange term since the bond of two electrons on the different orbits has a lower energy. The first term is the hopping term in the projected Hilbert space without double occupancy. The strong correlation should lead to different physics from that of free particles. To obtain the phase diagram, we use the Schwinger boson technique.[22–24] In the representation of the Schwinger boson for an orbital and fermions for charge, the Hamiltonian is rewritten as[15]

$$H_{\mathrm{eff}}=-t\sum_{ij}\ b^{\dagger}_{i,\alpha}b_{j,\alpha}f^{\dagger}_{i}f_{j}+\sum_{ij}\ \frac{t^2}{2U}(m_{i,\alpha}m_{j,\alpha}-n_in_j),$$

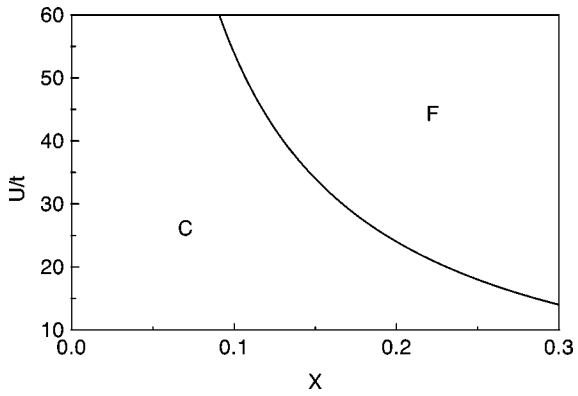

FIG. 4. The phase diagram for orbital ordering in low doped manganites: the strong-correlation approach.

where $m_{i,\alpha}=b^{\dagger}_{i,\alpha}b_{i,\alpha}-b^{\dagger}_{i,\bar{\alpha}}b_{i,\bar{\alpha}}$ and $n_i=b^{\dagger}_{i,\alpha}b_{i,\alpha}+b^{\dagger}_{i,\bar{\alpha}}b_{i,\bar{\alpha}}$. A local constraint for the orbital boson and charge fermion is

$$f^{\dagger}_i f_i=b^{\dagger}_{i,\alpha}b_{i,\alpha}+b^{\dagger}_{i,\bar{\alpha}}b_{i,\bar{\alpha}},$$

which can be realized by introducing the Lagrange multipliers in the Hamiltonian. To study the phase diagram, the simplest approach to the boson part of the Hamiltonian is the saddle-point approximation in which all the boson field and Lagrange multipliers are taken to be independent of time and space. Since we are interested in the orbital structure of the ground state, G-, C-, and A-type orderings are parametrized by decomposing the system in two sublattices *A* and *B*. F-type ordering is established if the two sublattices become identical. In the case of low dopings, we have

$$\langle b_{i,z}\rangle=\sqrt{1-x}\cos\frac{\alpha_{A(B)}}{2}$$

and

$$\langle b_{i,\bar{z}}\rangle=\sqrt{1-x}\sin\frac{\alpha_{A(B)}}{2}.$$

$\langle b_{i,z}\rangle$ and $\langle b_{i,\bar{z}}\rangle$ are determined by the sublattice structures. The mean-field phase diagram is obtained by minimizing the ground-state energy in terms of the two parameters α_A and α_B. At $x=0$, the band for fermions is fully filled and the hopping terms vanish. The ground-state energies per bond for both C- and G-type phases are $-t^2/2U$, while $\alpha_A=-\alpha_B=\pi/2$ for the C-type and $\alpha_A=\pi-\alpha_B$ for G-type. The C- and G-type orbital orderings are degenerated, in agreement with the results of spin-wave theory.[21,25] However, the C-type ordering was observed experimentally in the undoped case.[16] Hotta *et al.*[26] suggested that the cooperative Jahn-Teller effect leads to a C-type orbital structure. When the system deviates from the undoped case, the problem should be solved self-consistently. In this approach, we find that any small doping removes the degeneracy of C- and G-type orderings and the C-type structure has a lower energy. The hopping term in the projected Hilbert space favors forming a ferro-orbital phase, which is very similar to the double exchange model. When the doping increases, a phase transition from C-type ordering to F-type ordering occurs in the ground state at a finite x_c, which is a function of the ratio t/U, as shown in Fig. 4. Thus the competition between the hopping term and the superexchange term leads to the orbital phase transition.

V. DISCUSSIONS

Both Figs. 3 and 4 indicate a phase transition from C-type to F-type ordering. The starting points for these two figures are quite different: One is for weak correlations and the other is for strong correlations. If the system deviates from the spin ferromagnetic state and other spin structures are allowed, the C-type orbital ordering tends to form the spin A-type structure. This is because, from the superexchange mechanism, the nearest-neighbor bond has a lower energy if it is spin ferromagnetic and orbital antiferromagnetic or spin antiferromagnetic and orbital ferromagnetic.[27] This coincides with the magnetic structure in the undoped mangnite. The experimental phase diagram tells us that the layered FM insulating phase evolves into a ferromagnetic insulating state.[5,6] No obvious magnetic phase transition is observed until $x=0.175$. Thus the increment of doping weakens the spin AF correlation along the *c* axis, and does not change the orbital structure dramastically. The orbital ordering is C-type, not G-type at low dopings. It was observed that a transition occurs near $x=0.175$ in the ferromagnetic background. We believe that it is closely related to the transition discussed in this work. If we take $U/t=20$, the critical value x_c is about 0.23 in Fig. 4, which is larger than the experimental value. However, other physical effects, when they are properly taken into account, might reduce x_c. Yunoki *et al.*[12] studied the Jahn-Teller effect in an orbital model without on-site interaction. A phase transition of orbital ordering was also observed in their study for a strong electron-phonon interaction. We believe that the inclusion of the electron-phonon interaction could reduce the critical value x_c. Maezono *et al.*'s mean-field phase diagram contains a transition from the G-type to F-type phase.[11] Our RPA result also shows the instability from para-orbital phase to the G-type ordering phase when *U* is relatively small. It is worth mentioning that our theory is different from those of the polaron-ordering phase[28] and band polarization.[29] Generally speaking, once the long-range orbital ordering exists, the Jahn-Teller distortion always appears. A regular arrangement of orbitals, i.e., electron cloud, affects the structure of the system. So when the orbital phase transition from C- to F-type occurs, it is not surprising that the Jahn-Teller distortion also disappears. To explain the lattice distortion observed experimentally, one has to introduce the electron-phonon interaction. Even excluding the Coulomb interaction, the Jahn-Teller distortion alone can drive an orbital phase transition. However, it was already realized that the electron correlation is very strong in doped manganites. On-site Coulomb interactions are dominant and are sufficient to drive an orbital phase transition.

Before ending this paper, we would like to mention that the C-type orbital ordering does not necessarily imply an insulating phase. However, in the C-type structure, the orbitals of the electron tend to be parallel along the *c* axis and antiparallel in the *a*-*b* plane. Thus, electrons tend to move along the *c* axis as the hopping among the *a*-*b* plane will tend to destroy the orbital antiferromagnetic structure and is energetically costly. The electron energy band in the *a*-*b* plane is much narrower than that along the *c* axis. Thus the

high anisotropy of the C-type phase leads to an almost one-dimensional character for the energy band. In an ideal one-dimensional system, any amount of disorder will drive the system to be an insulator. There are always disorders in the system, for instance, spin fluctuations. Thus, the system with the C-type ordering is most likely an insulator. On the other hand, the orbital superexchange interaction in Eq. (1) is attractive for charge carriers. Usually, strong interaction (either repulsive or attractive) will cause a uniform density phase to be unstable, either against the Wigner lattice or phase separation. The antiferromagnetic orbital ordering will suppress the effective hopping term and relatively enhance the attraction such that it is possible to drive a uniform-density phase unstable at low dopings. This will lead to the phase separation senario for a metal-insulator transiton.[30,15] The resulting phase separation between two phases with different densities was observed near $x=0.05$ and 0.08.[31,32] As the physical origin of the phase separation here is a repulsive interaction, it seems to be a paradox since the repulsion is believed to prevent phase separation. This paradox can be resolved if one realizes that the interaction here is on-site and its only effect is to exclude the double occupancy of charge carriers. It has no obvious effect to prevent the system from forming two different density phases if both phases have excluded double occupancy already. The effective interaction drives charge carriers around to a lower energy by optimizing the orbital configurations. Similar physics was extensively discussed in the t-J model for high-temperature superconductivity.[33] In short, the C-type orbital ordering has a strong tendency to be an insulating phase.

In conclusion, a phase transition from the C-type to F-type orbital ordering occurs at low doping in the regime of strong correlations. This transition is relevant to the ferromagnetic metal-insulator transition in the lightly doped manganites at low temperatures.

ACKNOWLEDGMENTS

This work was supported by a RGC grant of Hong Kong, and the National Natural Science Foundation of China. X.C.X. was supported by the U.S.-DOE.

[1] S. Uhlenbruck *et al.*, Phys. Rev. Lett. **82**, 185 (1999).
[2] Y. Endoh *et al.*, Phys. Rev. Lett. **82**, 4328 (1999).
[3] H. Nojiri *et al.*, Phys. Rev. B **60**, 4142 (1999).
[4] Y. Tomioka *et al.*, Phys. Rev. Lett. **74**, 5108 (1995).
[5] Y. Tokura *et al.*, J. Phys. Soc. Jpn. **63**, 3931 (1994).
[6] P. Schiffer *et al.*, Phys. Rev. Lett. **75**, 3336 (1995).
[7] K. I. Kugel and D. I. Khomskii, Zh. Éksp. Teor. Fiz. **64**, 1429 (1973) [Sov. Phys. JETP **37**, 725 (1973)].
[8] J. Inoue and S. Maekawa, Phys. Rev. Lett. **74**, 3407 (1995).
[9] S. Ishihara, J. Inoue, and S. Maekawa, Physica C **263**, 130 (1996); S. Ishihara, M. Yamanaka, and N. Nagaosa, Phys. Rev. B **56**, 686 (1997).
[10] H. Shiba, R. Shiina, and A. Takahashi, J. Phys. Soc. Jpn. **66**, 941 (1997); R. Shiina, T. Nishitani, and H. Shiba, *ibid.* **66**, 3159 (1997).
[11] R. Maezono, S. Ishihara, and N. Nagaosa, Phys. Rev. B **57**, R13 993 (1998).
[12] S. Yunoki, A. Moreo, and E. Dagotto, Phys. Rev. Lett. **81**, 5612 (1998).
[13] P. Horsch, J. Jaklic, and F. Mack, Phys. Rev. B **59**, 6217 (1999).
[14] J. van den Brink and D. Khomskii, Phys. Rev. Lett. **82**, 1016 (1999).
[15] S. Q. Shen and Z. D. Wang, Phys. Rev. B **58**, R8877 (1998); **61**, 9532 (2000).
[16] Y. Murakami *et al.*, Phys. Rev. Lett. **80**, 1932 (1998); **81**, 582 (1998).
[17] J. C. Slater and G. F. Koster, Phys. Rev. **94**, 1498 (1954).
[18] P. B. Allen and V. Perebeinos, Phys. Rev. B **60**, 10 747 (1999).
[19] J. S. Griffith, *The Theory of Transition Metal Ions* (Cambridge University Press, Cambridge, UK, 1971).
[20] T. Mizokawa and A. Fujimori, Phys. Rev. B **54**, 5368 (1996).
[21] J. van der Brink, P. Horsch, F. Mack, and A. M. Oleś, Phys. Rev. B **59**, 6795 (1999).
[22] D. P. Arovas and A. Auerbach, Phys. Rev. B **38**, 316 (1988).
[23] S. K. Sarker, C. Jayaprakash, H. R. Krishnamurthy, and M. Ma, Phys. Rev. B **40**, 5028 (1989).
[24] R. Y. Gu, Z. D. Wang, S. Q. Shen, and D. Y. Xing, Phys. Rev. B **61**, 1211 (2000).
[25] R. Y. Gu, S. Q. Shen, Z. D. Wang, and D. Y. Xing, cond-mat/9908464 (unpublished).
[26] T. Hotta, S. Yunoki, M. Mayr, and E. Dogotto, Phys. Rev. B **60**, R15 009 (1999).
[27] From the Pauli exclusion principle, the superexchange mechanism prohibits the spin and orbital ferromagnetic correlation. [See S. Q. Shen and Z. D. Wang, Phys. Rev. B **59**, 3291 (1999).]
[28] Y. Yamada *et al.*, Phys. Rev. Lett. **77**, 904 (1996).
[29] R. Senis *et al.*, Phys. Rev. B **57**, 14 680 (1998).
[30] A. Moreo, S. Yuniki, and E. Dagotto, Science **283**, 2034 (1999).
[31] G. Allodi *et al.*, Phys. Rev. B **56**, 6036 (1997).
[32] M. Hennion *et al.*, Phys. Rev. Lett. **81**, 1957 (1998).
[33] For a review, see S. A. Kivelson and V. J. Emery, in *Strongly Correlated Electronic Materials: The Los Alamos Symposium, 1993*, edited by K. S. Bedell *et al.* (Addison-Wesley, Reading, MA, 1994).